NATIONAL ADVISORY COMMITTEE FOR AERONAUTICS

TECHNICAL NOTE 3807

CONVERSION OF INVISCID NORMAL-FORCE COEFFICIENTS IN

HELIUM TO EQUIVALENT COEFFICIENTS IN AIR

FOR SIMPLE SHAPES AT HYPERSONIC SPEEDS

By James N. Mueller

Langley Aeronautical Laboratory
Langley Field, Va.

NACA

Washington

October 1956

T

NATIONAL ADVISORY COMMITTEE FOR AERONAUT.

TECHNICAL NOTE 3807

CONVERSION OF INVISCID NORMAL-FORCE COEFFICIENTS IN

HELIUM TO EQUIVALENT COEFFICIENTS IN AIR

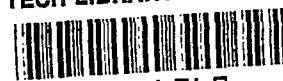FOR SIMPLE SHAPES AT HYPERSONIC SPEEDS

By James N. Mueller

SUMMARY

A simple correlation factor, based on inviscid shock-expansion cal-·culations for ideal-gas conditions, is found which permits conversion of the normal-force coefficients of simple shapes in helium to equivalent coefficients in air at Mach numbers of 12, 16, and 20. The results, although preliminary in nature, indicate that the conversion of exper-imental force data obtained in helium to equivalent data in air might not be overly complex and that hypersonic helium tunnels might be use-ful in conventional aerodynamic studies as well as in fundamental gas-dynamics studies.

INTRODUCTION

With the advent of the concept of hypervelocity vehicles, the Mach number range from 10 to 20 has become of more than academic interest; therefore, it is urgent that test facilities be developed which permit conventional aerodynamic studies at these high Mach numbers. The severe requirements of stagnation temperatures or pressures or both that must be met in order that wind tunnels using air may operate at Mach numbers of the order of 10 or greater has directed some attention toward the use of helium as a testing medium. (See, for example, ref. 1.) The use of helium, however, introduces a certain inherent disadvantage; namely, that the data obtained in helium are not directly equivalent to the data obtained in air because of the significant difference between the ratios of specific heats γ of the two gases. If the effects of this difference in the ratios of specific heats could be simply accounted for, the uti-lization of helium as a testing medium for conventional aerodynamic studies in hypersonic wind tunnels would be considerably strengthened. The usefulness of helium tunnels in fundamental gas-dynamics studies has already been demonstrated. (See ref. 2.)

The purpose of the present report is to obtain a preliminary insight into the effects of the ratio of specific heats γ from a nonviscous ideal-gas viewpoint and to try to account for these effects by use of a relatively simple correlation factor. As a basis for examining these effects, inviscid values of the normal-force coefficients of simple symmetrical shapes are computed for values of the ratio of specific heats of 7/5 for air and 5/3 for helium and are directly compared at Mach numbers of 12, 16, and 20. All computations of the airfoil surface pressures from which the normal-force coefficients are obtained are made by using the shock-expansion method. The computations are based on the assumption of ideal-gas flow and, therefore, preclude any effects of caloric and thermal imperfections on the flow properties. Also, viscous effects which were shown in tests reported in reference 2 to have a significant influence on the pressures on the forepart of sharp-edged configurations are likewise not considered. It is believed, however, that the omission of these effects will, in most cases, not seriously impair the usefulness of the comparative analysis presented herein. Therefore, the results should be indicative of the correlation that is possible.

SYMBOLS

A,B	constants in general equation for parabolic arc, $y = Ax - Bx^2$
c	chord
c_n	section normal-force coefficient, n/qc
c_p	specific heat at constant pressure
c_v	specific heat at constant volume
K,k	constants in point-slope form of equation for straight line, $y = Kx + k$
M	Mach number
n	section normal force
p	static pressure
q	dynamic pressure, $\dfrac{\gamma}{2} M^2 p$
t	maximum thickness

x   coordinate along X-axis

y   coordinate along Y-axis

α angle of attack, deg

C_1, C_2 characteristic coordinates (C_1 is positively inclined
                and C_2 is negatively inclined with respect to local
                velocity vector)

γ ratio of specific heats, c_p/c_v

δ angle of flow deflection, deg

θ half-angle at leading edge, deg

μ_∞ free-stream Mach angle, $\sin^{-1} \dfrac{1}{M_\infty}$

Subscripts:

∞ free stream

d   conditions just downstream of shock wave

m   mean

u   upper surface

He   in helium

Air   in air

METHOD OF ANALYSIS

The problem of obtaining exact formulas to represent the effects
of specific-heat ratio upon aerodynamic coefficients appears formidable
and was not considered to be within the scope of this paper. However,
one method of analysis which, although of a preliminary nature, appeared
to offer a means of obtaining some insight into the effects of the ratio
of specific heats γ was the direct comparison of calculated forces on
simple symmetrical shapes at the different values of γ. These com-
parisons would afford a basis upon which, it was hoped, a correlation
factor for the ratios of specific heats could be formulated. For sim-
plicity and because of a desire to obtain the most indicative cor-
relations, it was decided to make comparisons on a normal-force basis
only and to use the shock-expansion method as the means for obtaining

the pressure distributions (and, thus, the normal-force coefficients)
over the selected shapes.

CALCULATIONS

Theoretical Basis

The shock-expansion method (ref. 3) has been used extensively and
successfully in calculating flow about simple shapes traveling at super-
sonic speeds. As stated in reference 4, the method is a synthesis of
two basic mathematical tools for treating supersonic flows - namely,
the oblique shock equations of Meyer (ref. 5) and the corner expansion
equations of Prandtl and Meyer. An important attribute of the method
is its inherent advantage (over potential-flow theories) of accounting
for changes in entropy through shock waves. In this respect, then, the
shock-expansion method is especially well suited for treating hypersonic
flows about airfoils, inasmuch as these flows are usually characterized
by strong shock waves. However, the leading-edge shock wave interacts
with the Mach waves originating at the surface of an airfoil and this
interaction can appreciably alter the shape of the shock wave and the
flow downstream including the flow at the surface, especially in the
case of curved airfoils. Pertinent considerations at this point, then,
are the applicability and accuracy of the shock-expansion method for
predicting airfoil surface pressures in the Mach number range with which
this study is concerned. Therefore, a discussion of these factors is
included.

In a study by Eggers, Syvertson, and Kraus (ref. 6) of inviscid
flow about airfoils at high supersonic speeds, it was pointed out that
there is only one basic assumption underlying the shock-expansion method:
disturbances incident on the nose shock (or, for that matter, any other
shock) are consumed almost entirely in changing the direction of the
shock. Furthermore, the results of the study showed this basic assump-
tion to be essentially true. In figure 1 is shown the variation with

flow-deflection angle δ of the disturbance-strength ratio $\dfrac{\partial \delta}{\partial c_1} \Big/ \dfrac{\partial \delta}{\partial c_2}$

behind an oblique shock wave for various free-stream Mach numbers. (In
ref. 6 this ratio is considered as a measure of the ratio of the strengths
of the disturbances reflected from the shock wave to the disturbances
incident on the shock wave.) Figure 1(a) is computed for air $(\gamma = 7/5)$
and figure 1(b) for helium $(\gamma = 5/3)$. Reference 6 and figure 1(a) show
that except at extremely large deflection angles (close to those for
shock detachment) the ratio for air is small (in absolute value) com-
pared with 1 throughout the Mach number range considered. The present

calculations show that the ratio for helium (fig. 1(b)) is, by compar-
ison, even smaller (excluding, as for air, the angles close to shock
detachment). Thus, it is indicated that almost all of an incident dis-
turbance is generally absorbed in the shock wave for helium as well as
for air; and, as pointed out in reference 6, the flow along the stream-
lines is essentially of the Prandtl-Meyer type. Therefore, this result
substantiates the basic assumption of the shock-expansion method and
yields additional credence to the method for application to high Mach
numbers. If, on the basis of these findings, a maximum absolute value
for $\dfrac{\partial \delta}{\partial c_1} \Big/ \dfrac{\partial \delta}{\partial c_2}$ of 0.06 is chosen for air, the region in which the shock-
expansion method is applicable can readily be obtained from figure 1.
(This value of 0.06 is identical with that chosen in reference 6 for air.
A much lower value for $\dfrac{\partial \delta}{\partial c_1} \Big/ \dfrac{\partial \delta}{\partial c_2}$ could have been chosen for helium, based
on calculations made herein and as shown in fig. 1(b).) The upper bound-
ary line of this region is shown in figure 2, and it is evident that it
lies only slightly below (about 1° to 2°, in general) the line corre-
sponding to shock detachment which is given approximately by the line
for $M_1 = 1.0$. Almost the entire region of completely supersonic (ideal
gas) flow is then covered by the method. (See hatched area in fig. 2.)

Scope

    The section shapes for which computations of normal-force coeffi-
cients were made are shown in figure 3. The sections shown in fig-
ure 3(a) are 10-percent-thick slabs with parabolic-arc noses and were
selected as being crudely representative - with the probable exception
of the sharp leading edge - of possible hypersonic airfoil configurations.
The wedge slab sections (fig. 3(b)), on the other hand, were used to
examine the possibility of substituting these sections for the parabolic-
arc slab sections. The basis and justification of this substitution
are explained in this section.

    The concept of the Newtonian impact theory of fluid dynamics
($\gamma = 1$, $M_\infty = \infty$) is presented in reference 7 and is based on the hypoth-
esis that finite pressures are generated only on those airfoil surfaces
which "see" the flow. Analogously, the normal force on an airfoil
moving at hypersonic speeds is found to be determined almost entirely
by the pressure acting on the windward ("seeing") surface. Conversely,
the contribution of the leeward pressures is almost negligible. Examples
of this phenomenon at free-stream Mach numbers of 12, 16, and 20 are
given in figures 4 to 6, respectively, where the small effects of the
upper-surface (in this case, the leeward) pressures on the normal-force
coefficients of a flat plate are shown as a function of angle of attack.

It is evident that the lower-surface (in this case, the windward) pressures quickly become, with only a small increase in angle of attack from zero, the dominant factor in determining the normal-force coefficients. Thus, since the normal-force coefficients at other than small values of α are almost wholly dependent in the hypersonic range on the surface overpressures, it seems probable that the parabolic-arc slab airfoil section (fig. 3(a)) could be effectively represented (at least insofar as normal force is concerned) by a straight-line-element profile which successfully duplicates the average magnitude of the overpressures obtained on the original airfoil. This characteristic proves to be essentially true when the leading-edge half-angle and thickness of the wedge slab airfoil duplicate that of the parabolic-arc slab airfoil.

The merits of this substitution of airfoil shapes are immediately apparent in that (1) it appears possible to replace a curved-surface airfoil with a simple straight-line-element airfoil section and obtain theoretically comparable normal-force coefficients and (2) the theoretical calculations become greatly simplified.

The two parabolic-arc slab sections employed (fig. 3(a)) have different nose sizes (determined by the leading-edge half-angle θ) in order that the nose-bluntness effects on the correlation factor for the ratio of specific heats might be compared with those obtained for the wedge slab airfoils. The magnitudes of the leading-edge half-angles, on the other hand, were fixed by the relation $\theta = \delta_{M_d=1} - \alpha$, where $\delta_{M_d=1}$ is the angular deflection of the flow across an oblique shock to give $M_d = 1$, and α is the arbitrarily chosen maximum angle of attack of the configuration.

Calculations on the wedge slab configurations were made for eight leading-edge half-angles θ (as indicated in fig. 3(b)) in order to ascertain the effects of nose bluntness on the correlation factor. Leading-edge half-angles corresponding to those of the parabolic-arc slab configurations were also included in the calculations.

Computations were made at free-stream Mach numbers of 12, 16, and 20 for air ($\gamma = 7/5$) and for helium ($\gamma = 5/3$). Throughout the analysis the calculations were made within limits wherein the assumption was that the disturbed flow was everywhere supersonic, and, thus, that the shock wave was attached to the leading edge of the airfoils.

DISCUSSION

Some typical results of the inviscid normal-force calculations made by means of the shock-expansion method (which considers the pressures

on all surfaces of the airfoil) for the wedge slab configurations in helium and in air are shown in figures 7 to 9 for several representative leading-edge half-angles θ and at free-stream Mach numbers of 12, 16, and 20, respectively. The correlation factor K, which relates the helium data to the air data, is formulated from plots of this type and in the manner described in this section.

A comparison of the normal-force curves for air and for helium was made on the basis of an equal value of c_n $\left(\frac{c_{n,\text{Air}}}{c_{n,\text{He}}} = 1\right)$, as shown by the dashed lines in the plots of the variation of c_n with α. The results obtained from this comparison (which are the angles of attack required of the airfoil in air $\left(\alpha_{\text{Air}}\right)$ and in helium $\left(\alpha_{\text{He}}\right)$ to produce the same normal-force coefficient) are shown plotted as circles (arbitrarily chosen, representative data points) on the companion plots of the variation of α_{Air} with α_{He}. Further, it is shown that the variation of α_{Air} with α_{He} $\left(\text{for } \frac{c_{n,\text{Air}}}{c_{n,\text{He}}} = 1\right)$ can be closely approximated by the general slope-intercept equation of the form $y = Kx + k$. The curve which approximates the data is faired through the origin because in the limit when $c_n = 0$, $\alpha_{\text{Air}} = \alpha_{\text{He}} = 0^\circ$. Therefore, the intercept term k in the general equation need not be considered, and the conversion now depends merely on the factor K.

Figures 10 and 11 are representative plots at $M_\infty = 16$ which show the quantitative similarity which exists between the normal forces and the correlation curves obtained on the parabolic-arc slab sections and those obtained on the wedge slab sections with identical nose angles ($\theta = 11.27^\circ$ and $\theta = 24.27^\circ$, respectively) and thickness ratios. Comparable similarity is found to exist at the other Mach numbers ($M_\infty = 12$ and $M_\infty = 20$) for which calculations were made.

A tabulation and plot of the values of the correlation factor K are shown in figure 12 for all Mach numbers M_∞, leading-edge half-angles θ, and airfoil-section shapes. Strikingly evident is the small change or lack of change in the magnitudes of the correlation factors with section shape and with Mach number for a given value of θ. The use of the mean values of K (average value for the three Mach numbers), as shown plotted in the lower half of figure 12, insures acceptable accuracy.

Although this analysis has been made on the basis of airfoil-section data (or infinite-aspect-ratio conditions), there is reason to believe that the correlation factor would, in most cases, be applicable to three-dimensional bodies (for example, see ref. 4) when it is realized that the Mach angle μ_∞ at $M_\infty = 12$ is only 4.78°; at $M_\infty = 20$, μ_∞ becomes 2.87°.

CONCLUDING REMARKS

Based upon calculations employing the shock-expansion method and the assumption of ideal-gas conditions, a simple correlation factor is found which permits conversion of inviscid normal-force coefficients of simple shapes at Mach numbers of 12, 16, and 20 in helium to equivalent coefficients in air. The results, although preliminary in nature, indicate that the conversion of experimental force data obtained in helium to equivalent data in air might not be overly complex and that hypersonic helium tunnels might be useful in conventional aerodynamic studies as well as in fundamental gas-dynamics studies.

Langley Aeronautical Laboratory,
      National Advisory Committee for Aeronautics,
            Langley Field, Va., June 18, 1956.

REFERENCES

1. Bogdonoff, S. M., and Hammitt, A. G.: The Princeton Helium Hypersonic Tunnel and Preliminary Results Above M = 11. WADC Tech. Rep. 54-124, Wright Air Dev. Center, U. S. Air Force, July 1954.

2. Bogdonoff, Seymour M., and Hammitt, Andrew G.: Fluid Dynamic Effects at Speeds From M = 11 to 15. Jour. Aero. Sci., vol. 23, no. 2, Feb. 1956, pp. 108-116, 145.

3. Epstein, Paul S.: On the Air Resistance of Projectiles. Proc. Nat. Acad. Sci., vol. 17, no. 9, Sept. 1931, pp. 532-547.

4. Eggers, A. J., Jr., Savin, Raymond C., and Syvertson, Clarence A.:- The Generalized Shock-Expansion Method and Its Application to Bodies Traveling at High Supersonic Air Speeds. Jour. Aero. Sci., vol. 22, no. 4. Apr. 1955, pp. 231-238, 248.

5. Meyer, Th.: The Two Dimensional Phenomena of Motion in a Gas Flowing at Supersonic Velocity. Cornell Aero Lab., Aug. 1945. (Über zweidimensionale Bewegungsvorgänge in einem Gas das mit Überschallge-schwindigkeit strömt. Forsch.-Arb. Geb. Ing.-Wes., VDI-Verlag G.m.b.H., Heft. 62, 1908, pp. 31-67.)

6. Eggers, A. J., Jr., Syvertson, Clarence A., and Kraus, Samuel: A Study of Inviscid Flow About Airfoils at High Supersonic Speeds. NACA Rep. 1123, 1953. (Supersedes NACA TN 2646 by Eggers and Syvertson and NACA TN 2729 by Kraus.)

7. Busemann, A.: Flüssigkeits- und Gasbewegung. Handwörterbuch der Naturwissenschaften, Zweite Auflage (Gustav Fischer, Jena), 1933, pp. 244-279.
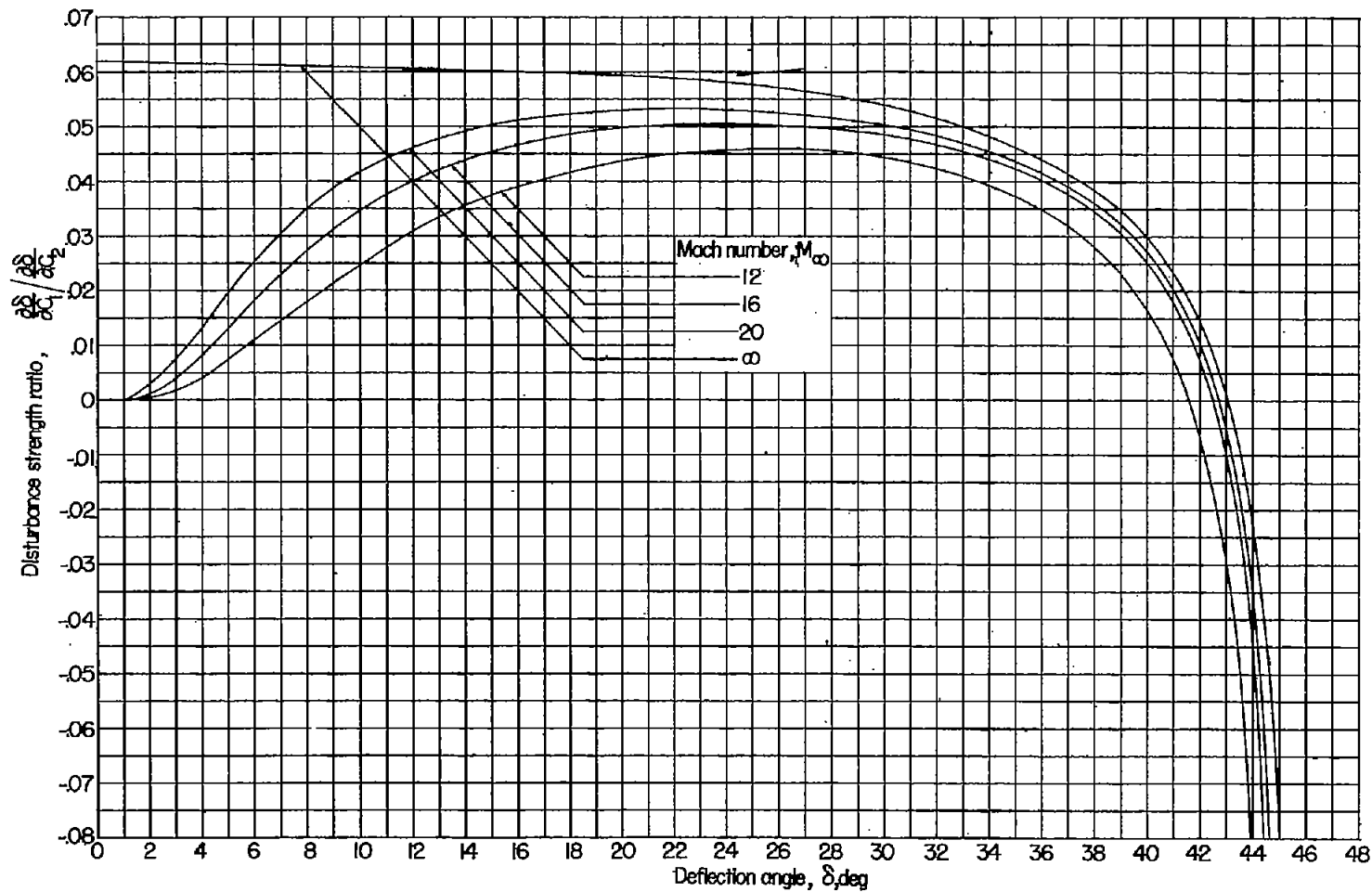
(a) Air; $\gamma = 7/5$.

Figure 1.- Variation with deflection angle of the disturbance strength
ratio behind an oblique shock wave for various free-stream Mach numbers.
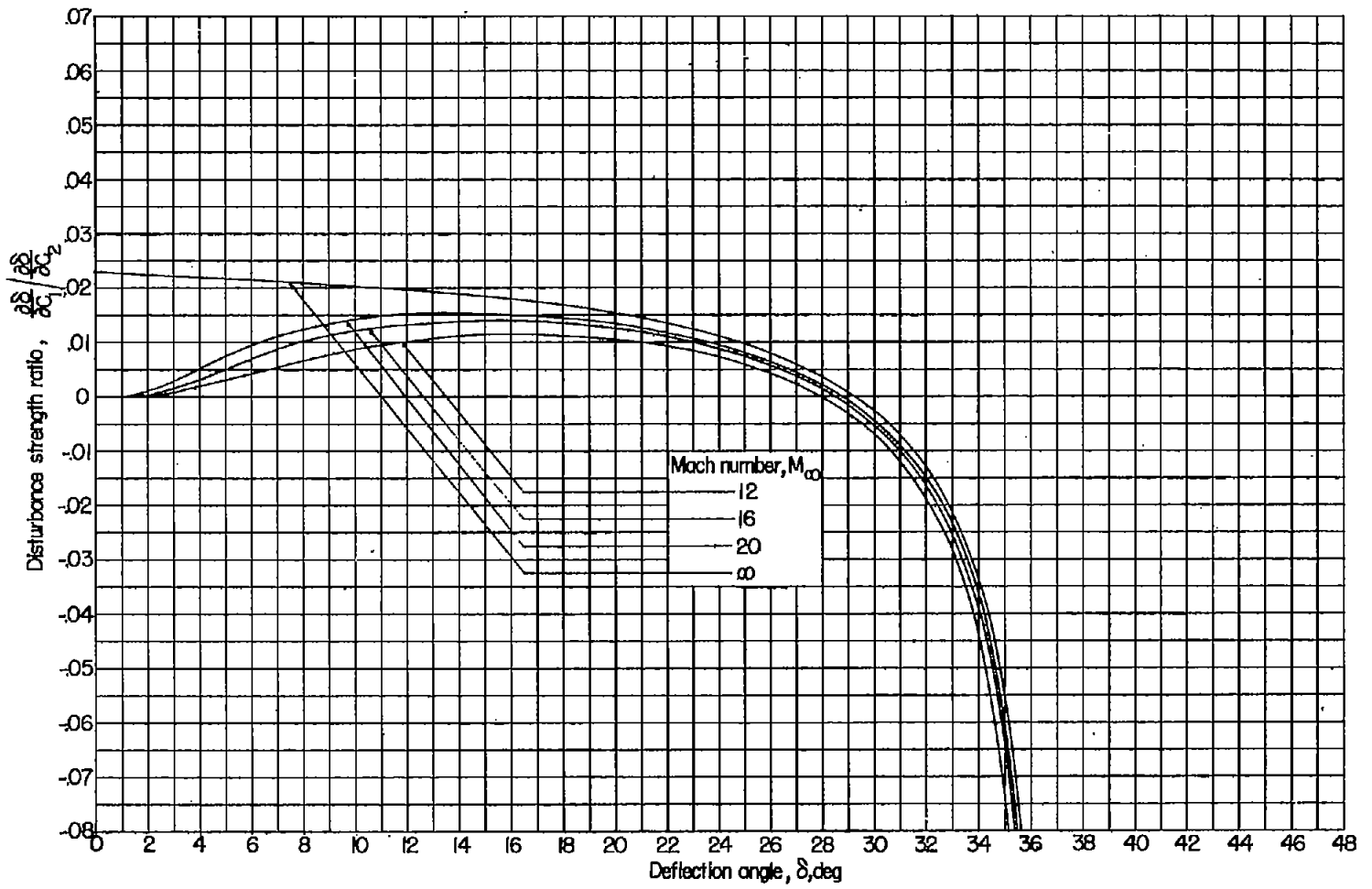
(b) Helium; $\gamma = 5/3$.

Figure 1.- Concluded.
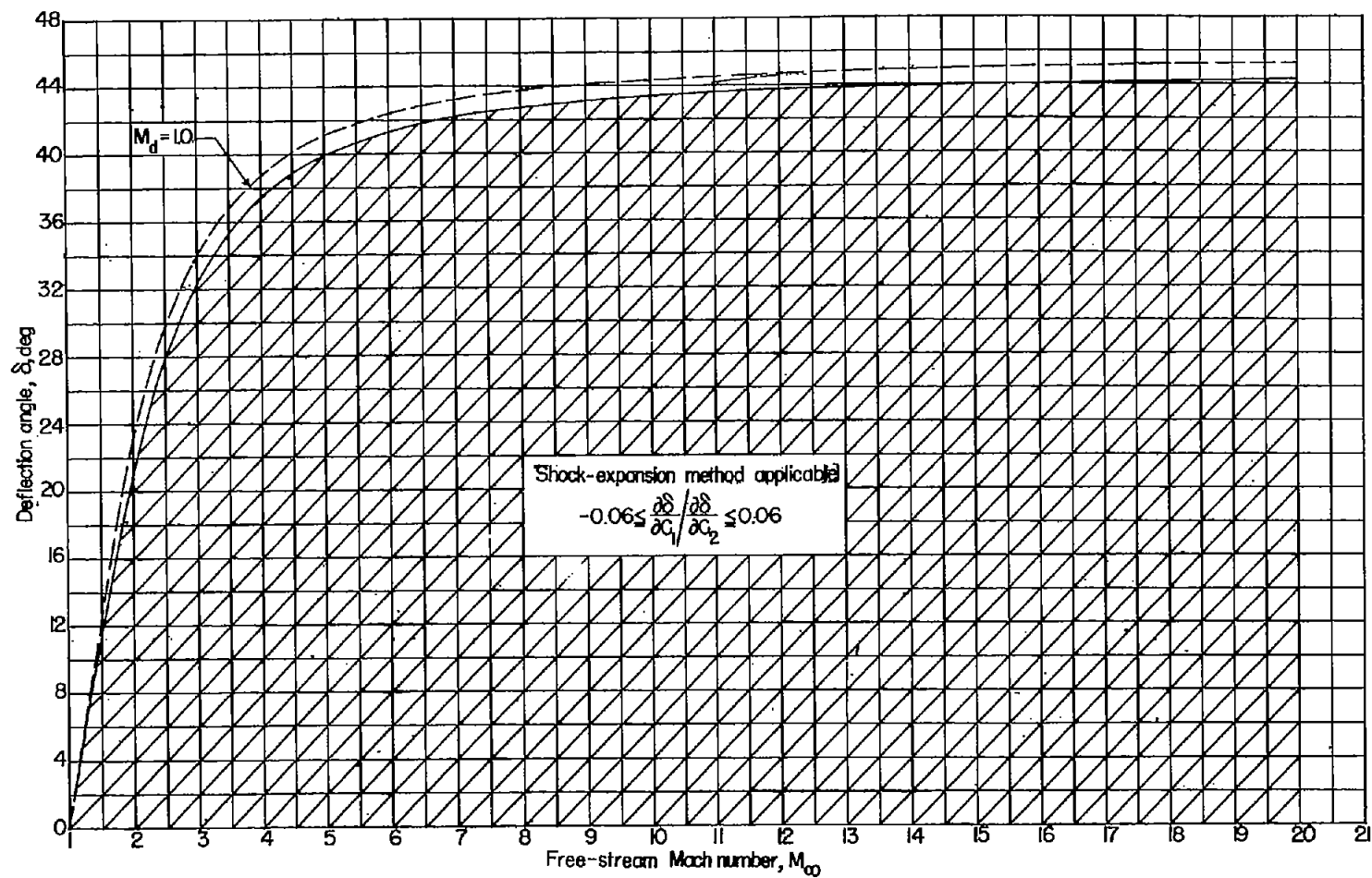
(a) Air; $\gamma = 7/5$.

Figure 2.- Range of applicability of shock-expansion method.

The graph shows Deflection angle, δ, deg (vertical axis, 0 to 48) versus Free-stream Mach number, M_∞ (horizontal axis, 0 to 21).

$M_d = 1.0$

Shock-expansion method applicable

$$-0.06 \leqq \frac{\partial \delta}{\partial C_1} \bigg/ \frac{\partial \delta}{\partial C_2} \leqq 0.06$$
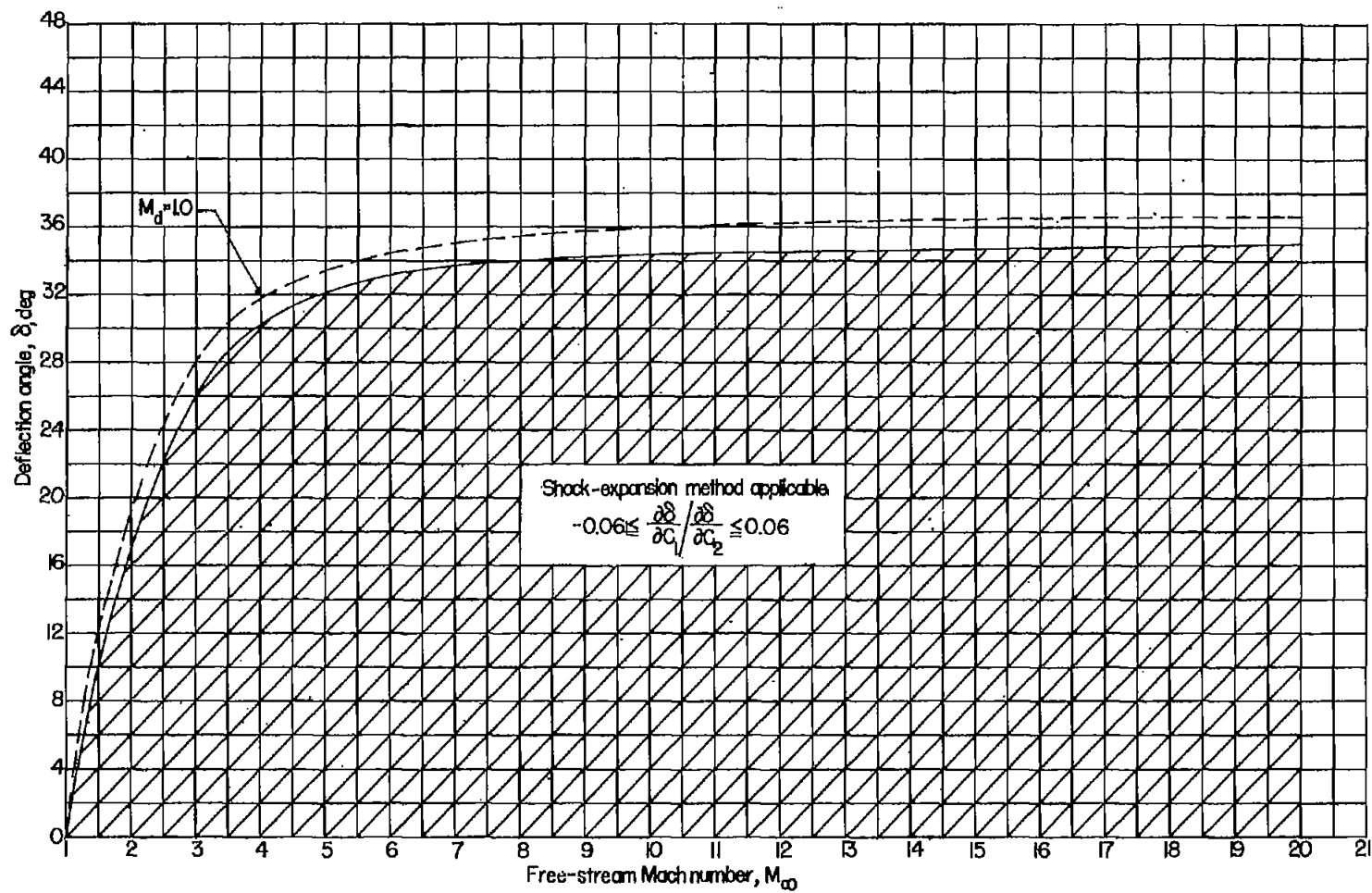
(b) Helium; $\gamma = 5/3$.

Figure 2.- Concluded.

$\theta = 11.27°$

$\theta = 24.27°$
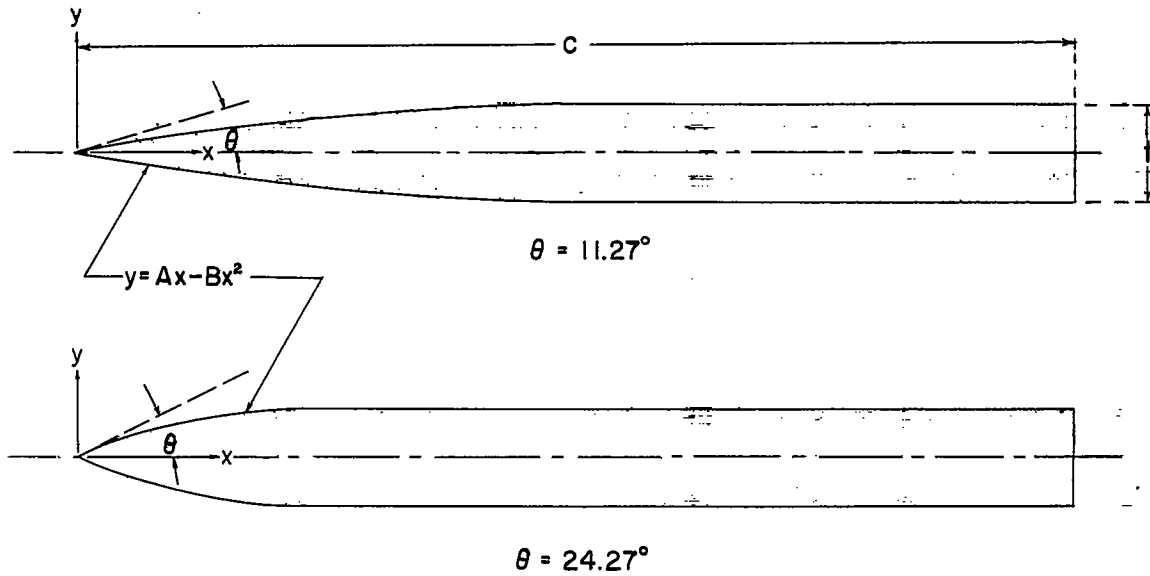
(a) Parabolic-arc slab airfoil section.

$\theta = 3°, 9°, 11.27°, 15°, 21°, 24.27°, 27°, 30°$
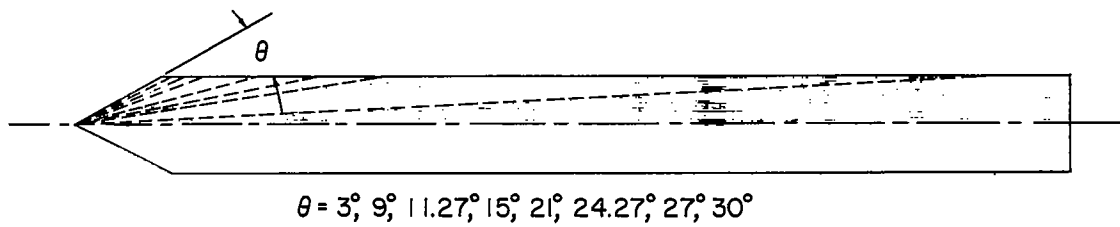
(b) Wedge slab airfoil section.

Figure 3.- Geometric shapes for which calculations of normal-force coefficients were made. Thickness, 10 percent.
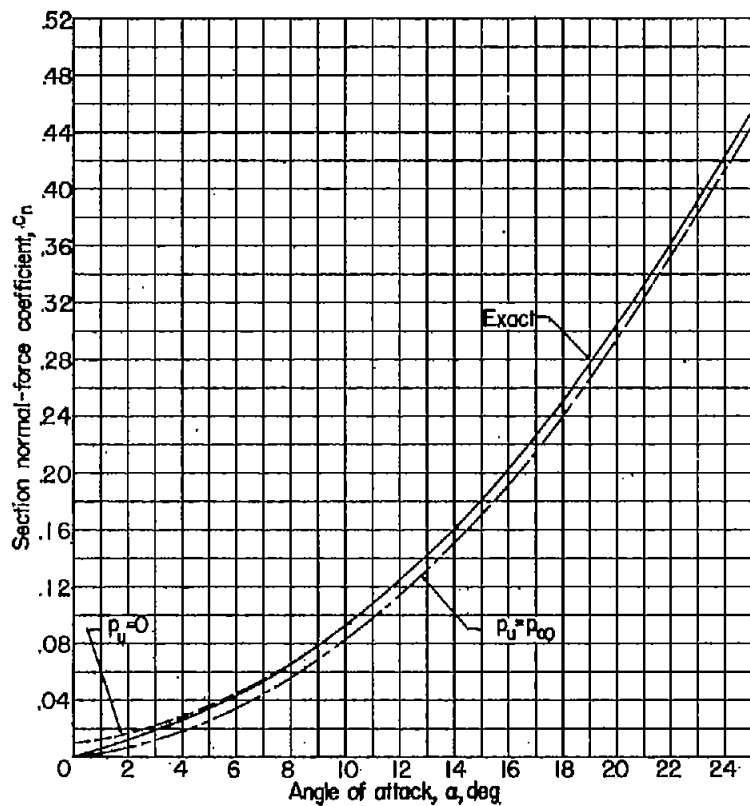
(a) Air; $\gamma = 7/5$.
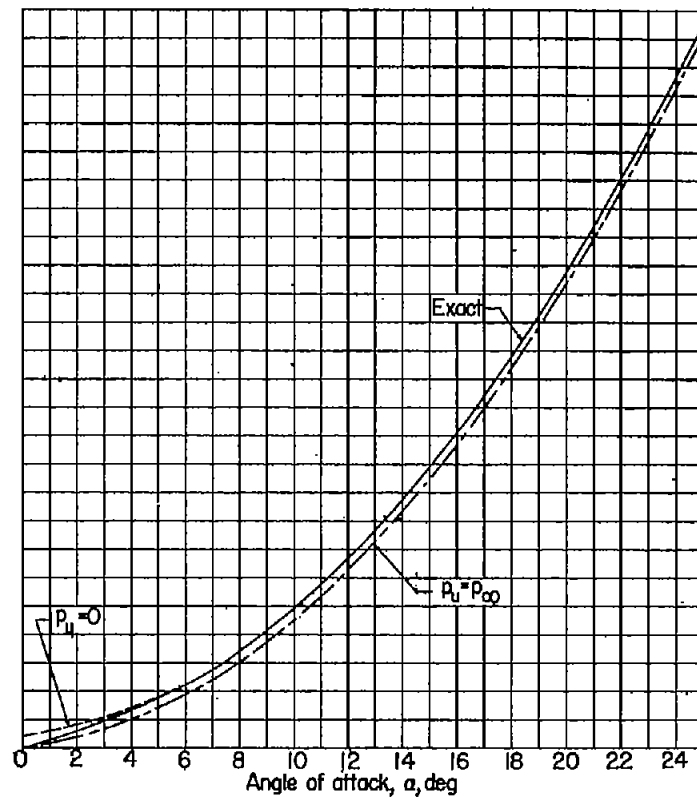
(b) Helium; $\gamma = 5/3$.

Figure 4.- Variation of flat-plate section normal-force coefficient with angle of attack at $M_\infty = 12$.
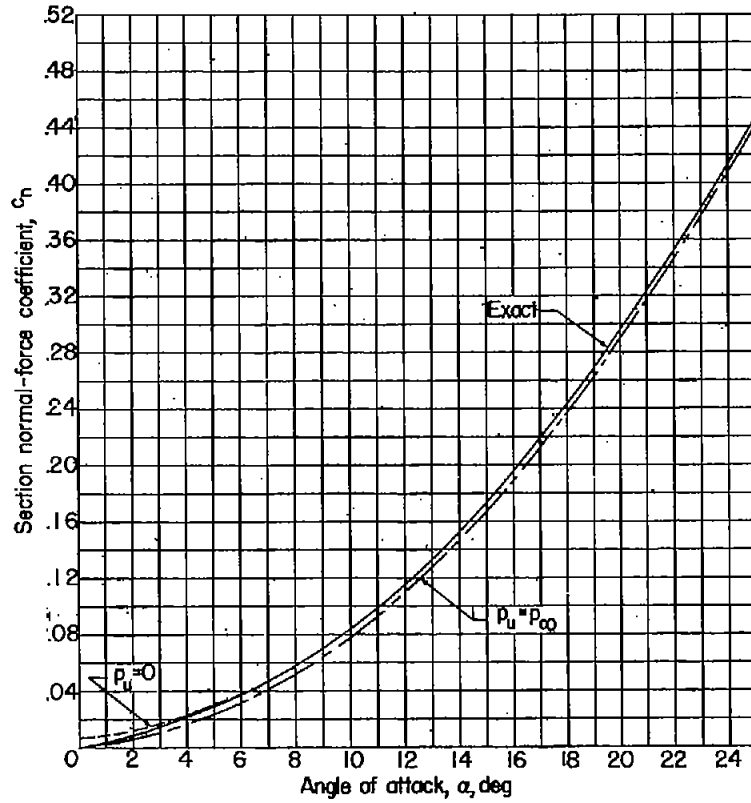
(a) Air; $\gamma = 7/5$.
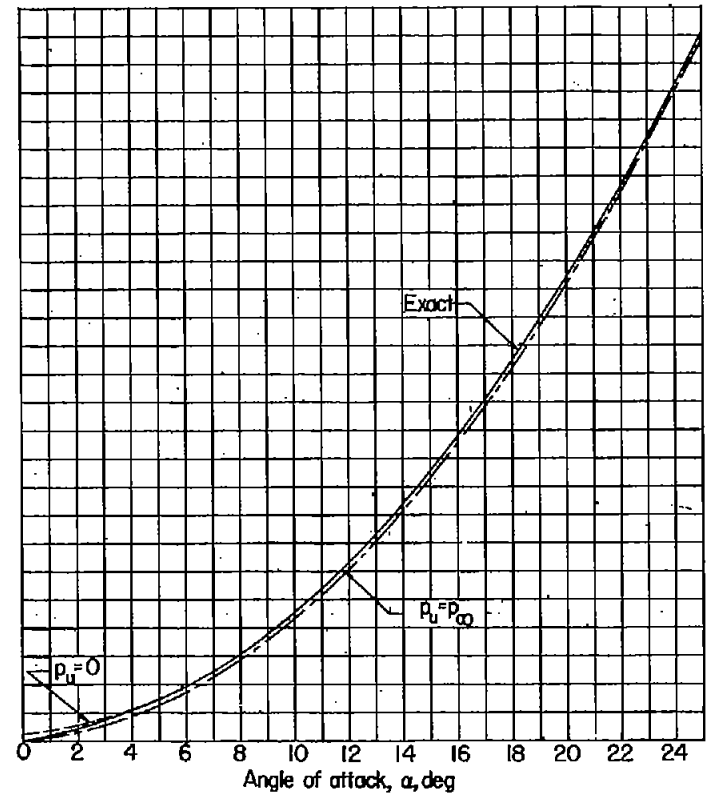
(b) Helium; $\gamma = 5/3$.

Figure 5.- Variation of flat-plate section normal-force coefficient with angle of attack at $M_\infty = 16$.
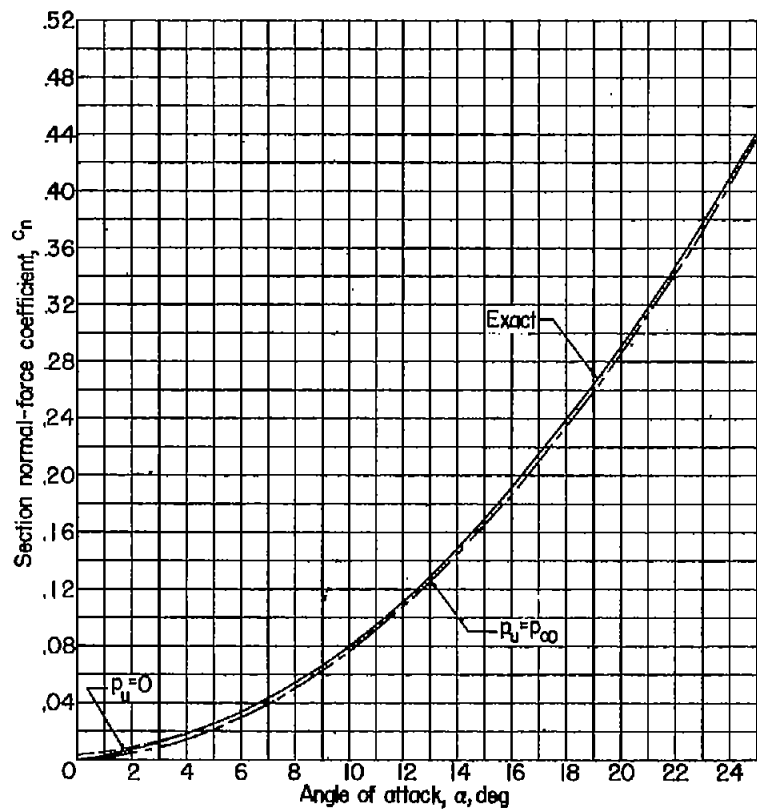
(a) Air; $\gamma = 7/5$.
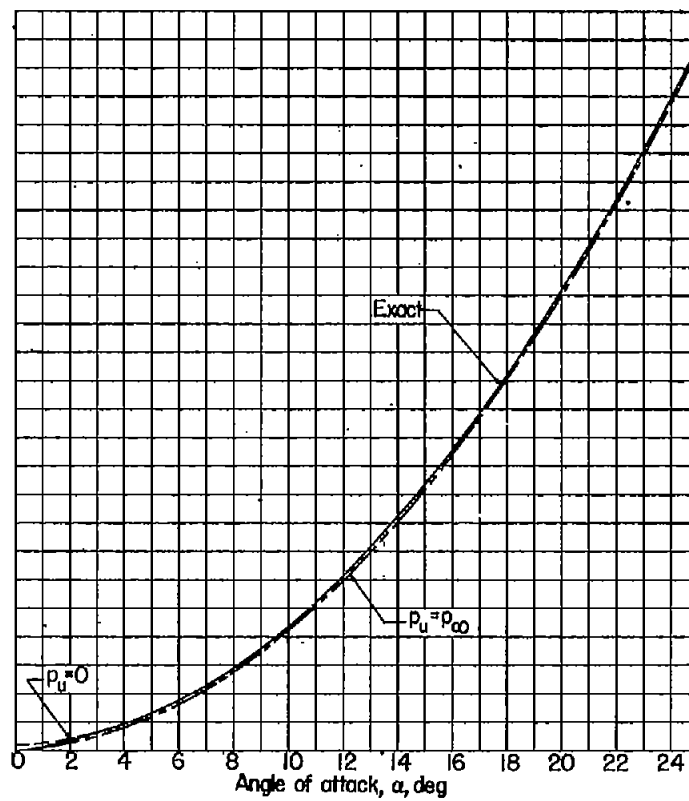
(b) Helium; $\gamma = 5/3$.

Figure 6.- Variation of flat-plate section normal-force coefficient with angle of attack at $M_\infty = 20$.

Section normal-force coefficient, c_n

.68
.64
.60
.56
.52
.48
.44
.40
.36
.32
.28
.24
.20
.16
.12
.08
.04

Helium

Criteria for obtaining representative data points

Air

0 2 4 6 8 10 12 14 16 18 20 22 24
Angle of attack, α, deg

Angle of attack in air, α_{Air}, deg

34
32
30
28
26
24
22
20
18
16
14
12
10
8
6
4
2

Locus of equation of the form, $y = Kx + k$

Representative data points

$\circ \ \dfrac{c_{n,Air}}{c_{n,He}} = 1$

0 2 4 6 8 10 12 14 16 18 20 22 24
Angle of attack in helium, α_{He}, deg

(a) $\theta = 0^\circ$ (flat plate).

Figure 7.- Variation of section normal-force coefficient c_n with angle of attack α and variation of α_{Air} with α_{He} for $c_{n,Air}/c_{n,He} = 1$ for various half-angles at leading edge for wedge slab airfoil sections at $M_\infty = 12$.
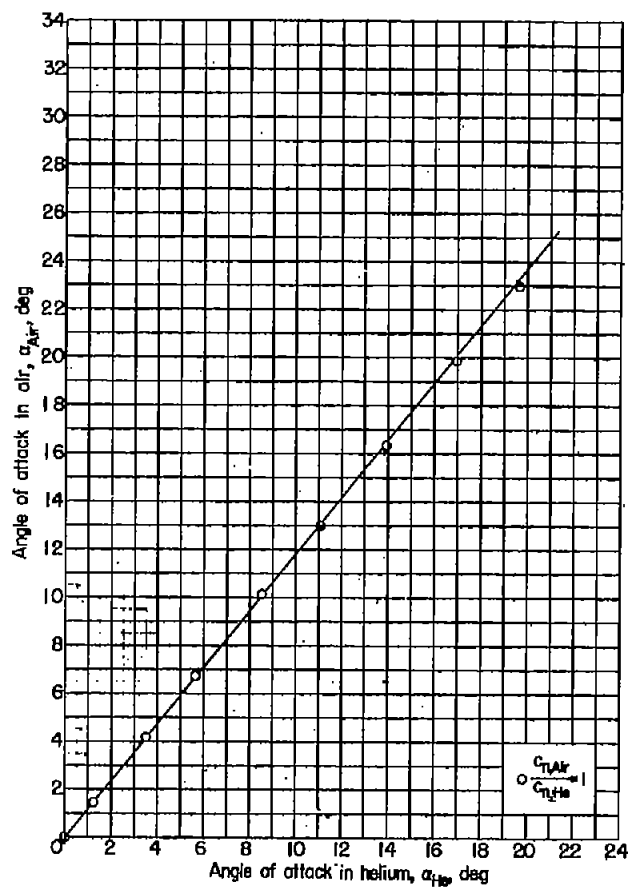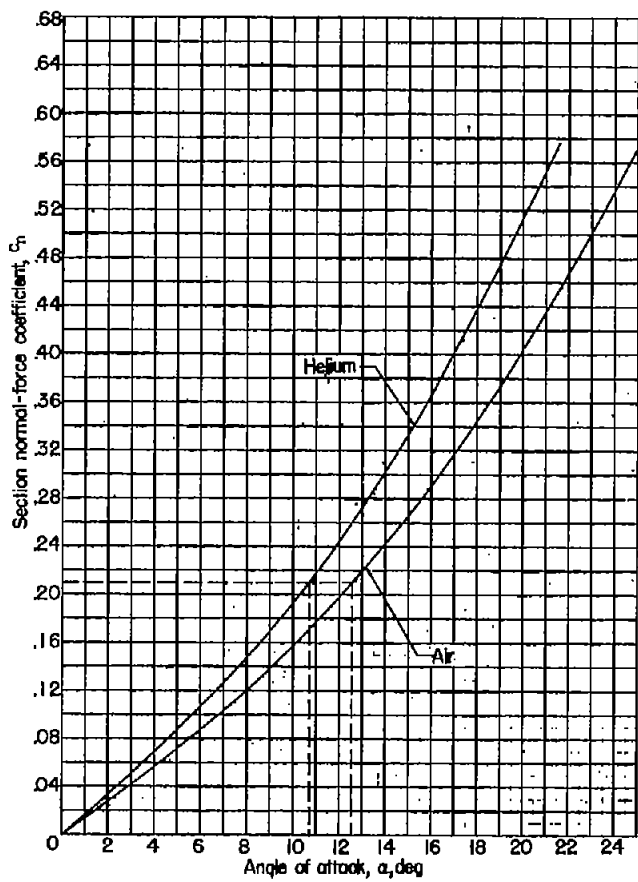
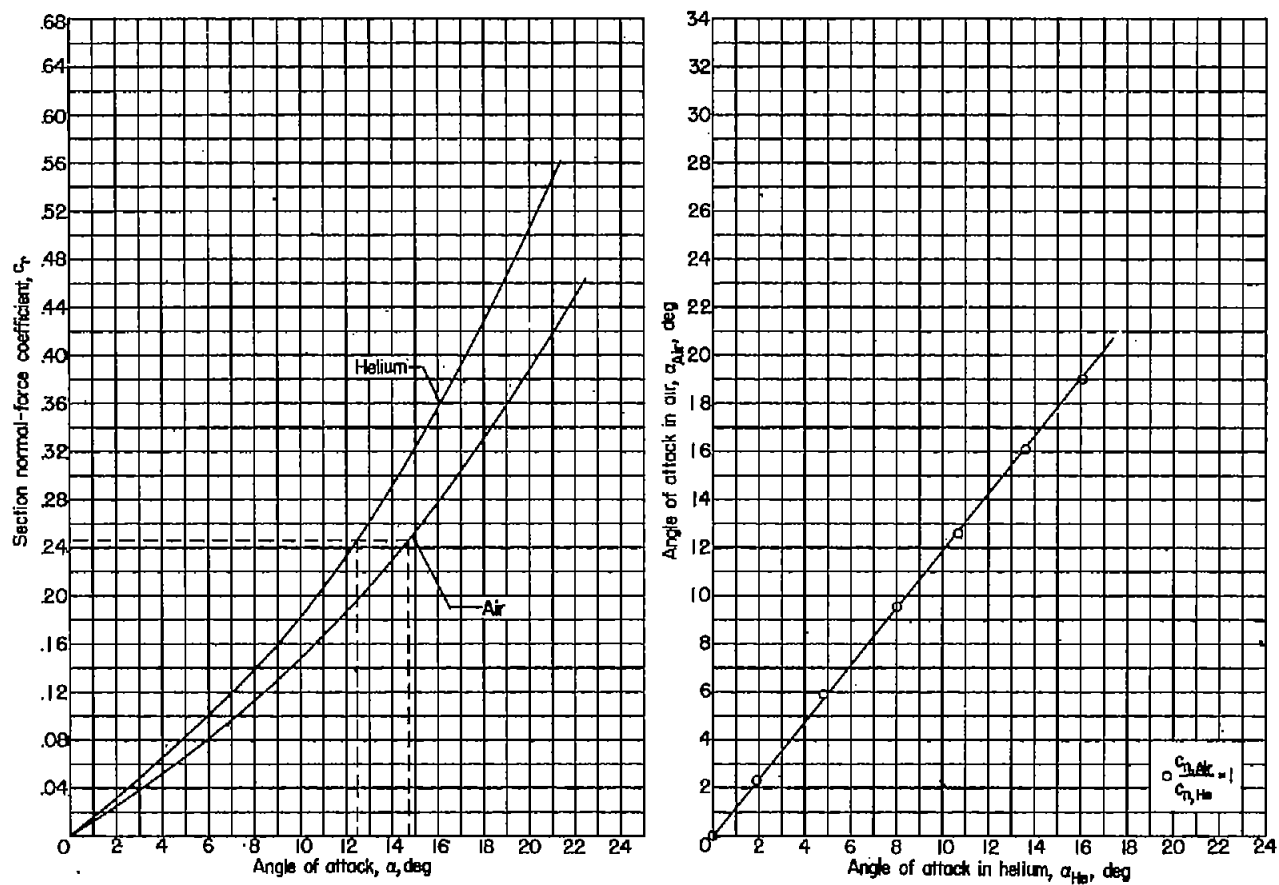(b) $\theta = 15^{\circ}$.

Figure 7.- Continued.
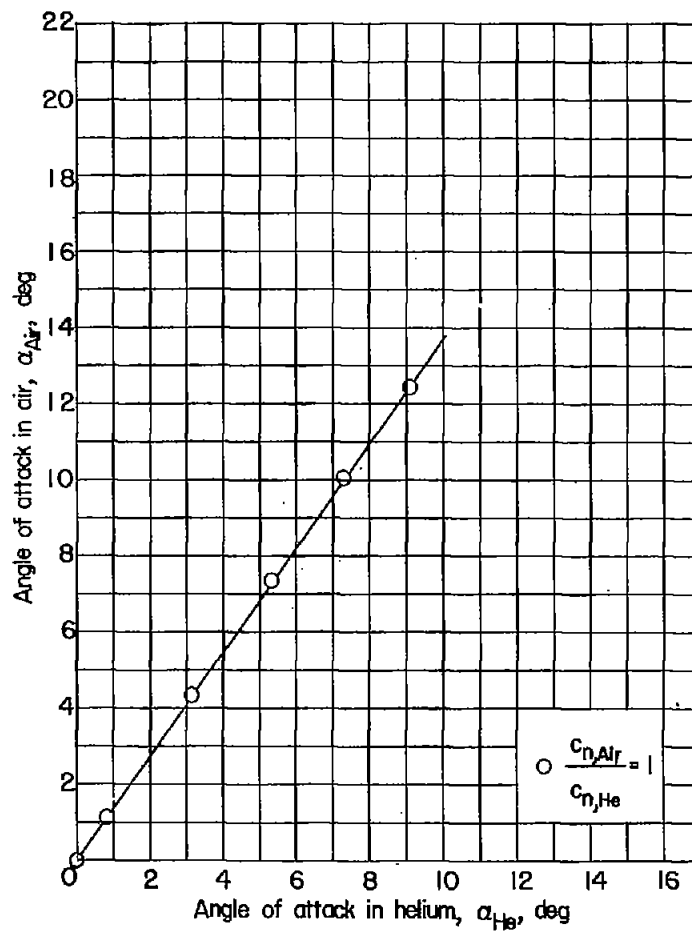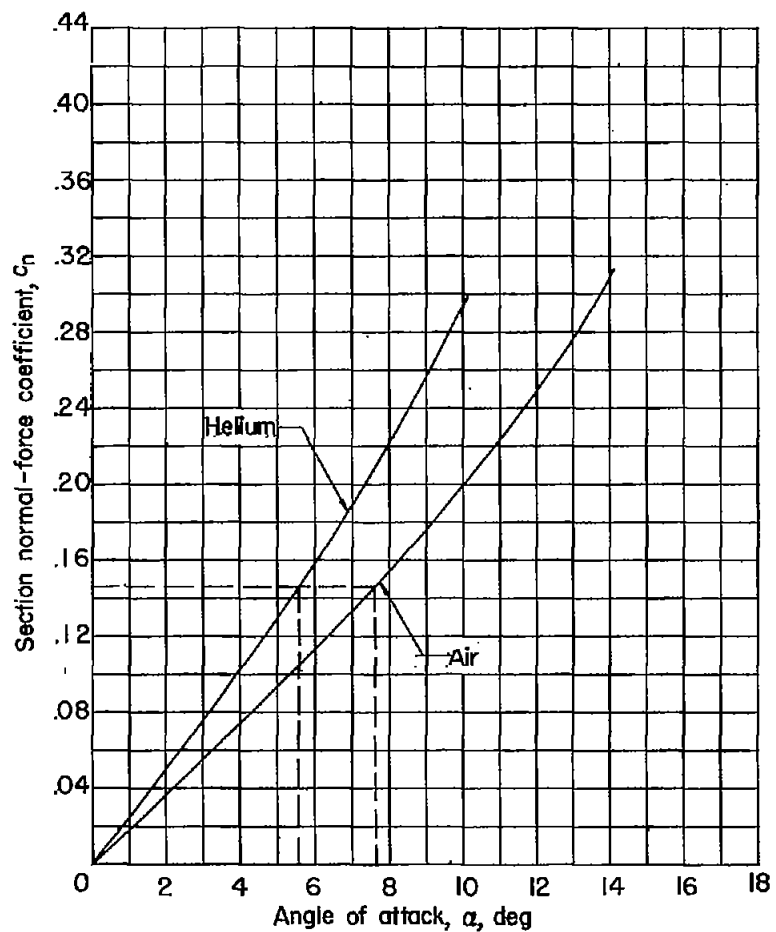
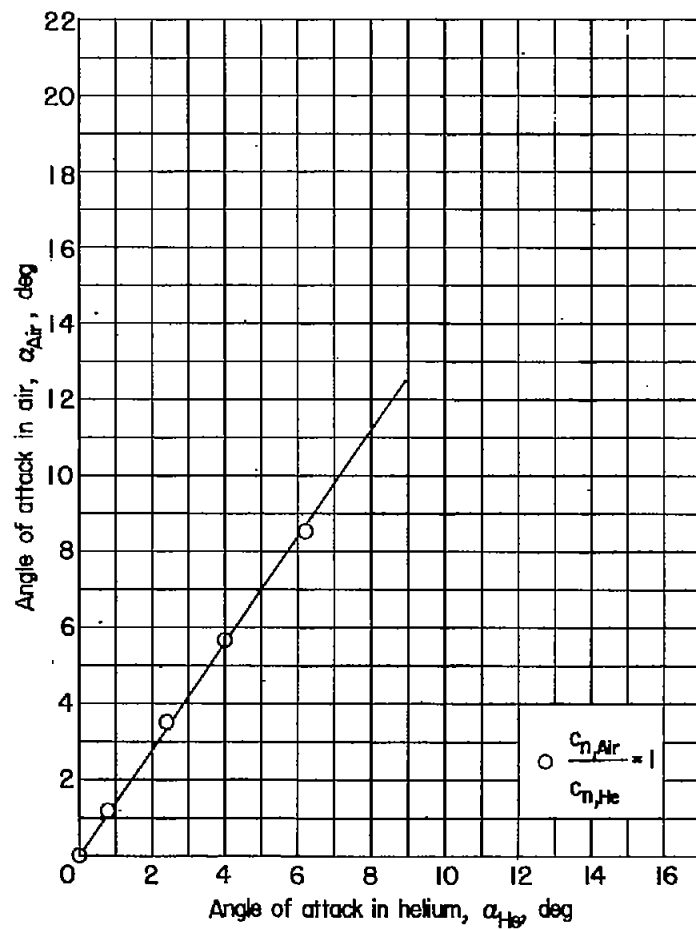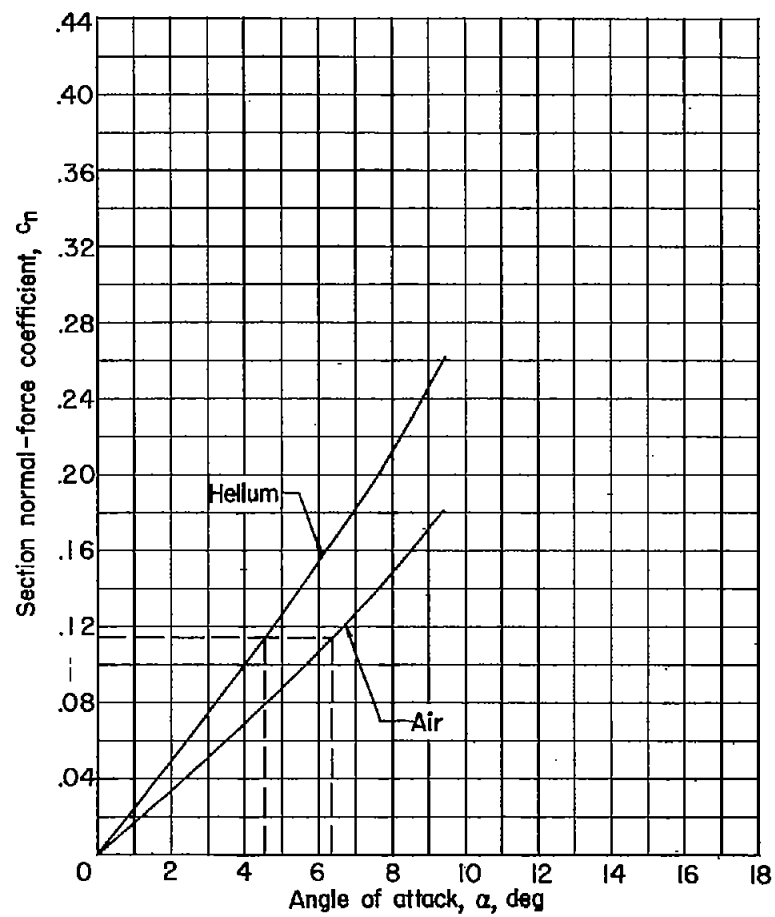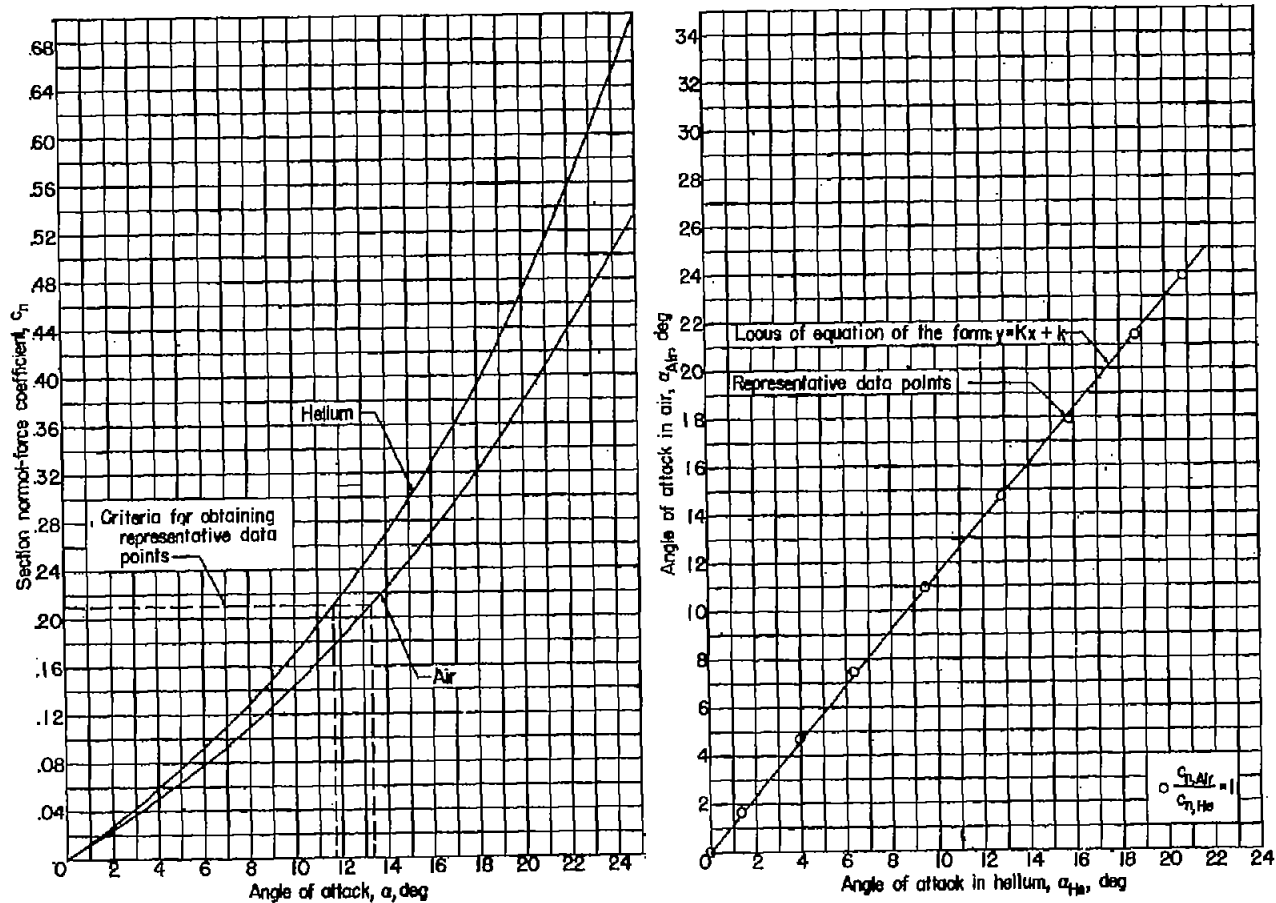(c) $\theta = 27^\circ$.

Figure 7.- Concluded.
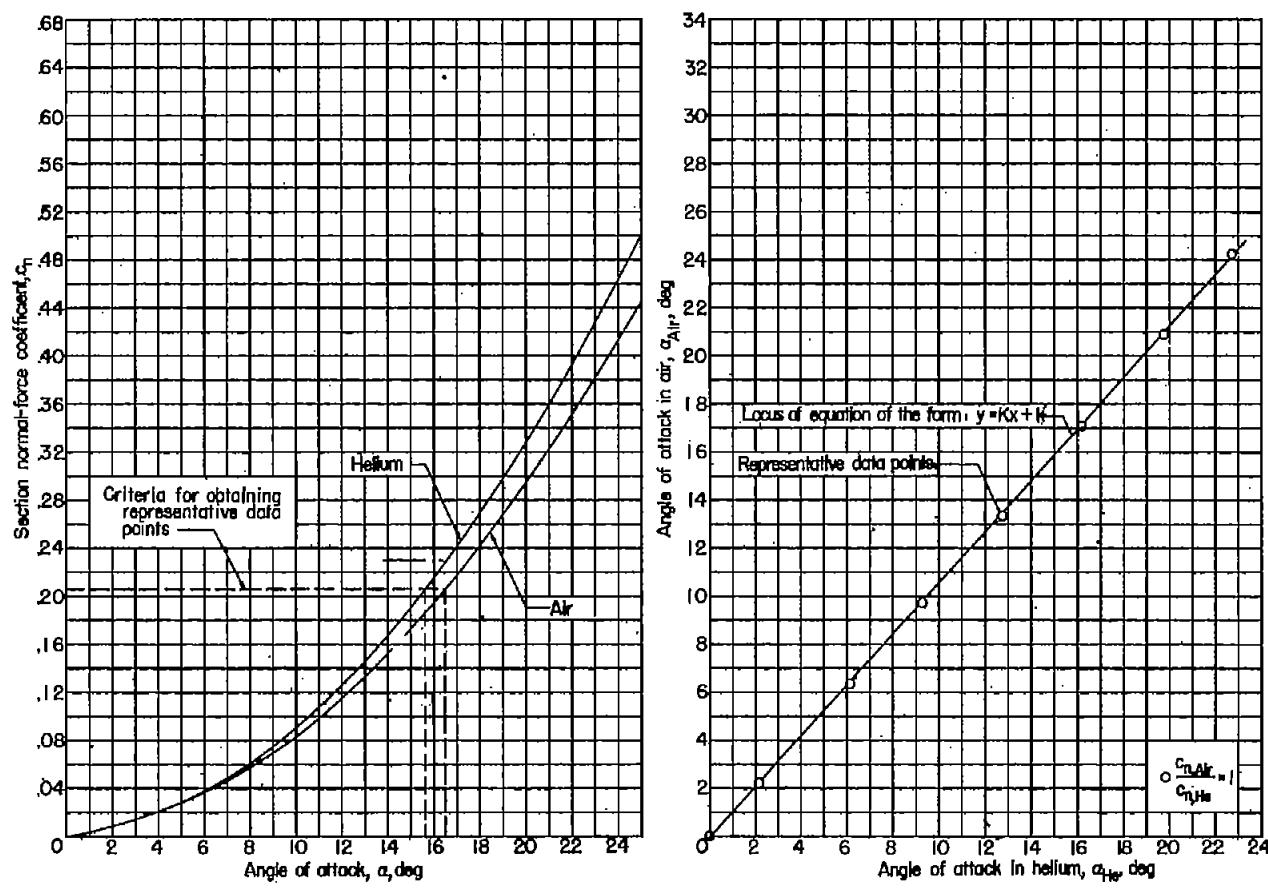
(a)   θ = 0° (flat plate).

Figure 8.- Variation of section normal-force coefficient c_n with angle of attack α and variation of α_{Air} with α_{He} for $c_{n,Air}/c_{n,He} = 1$ for various half-angles at leading edge for wedge slab airfoil sections at $M_\infty = 16$.
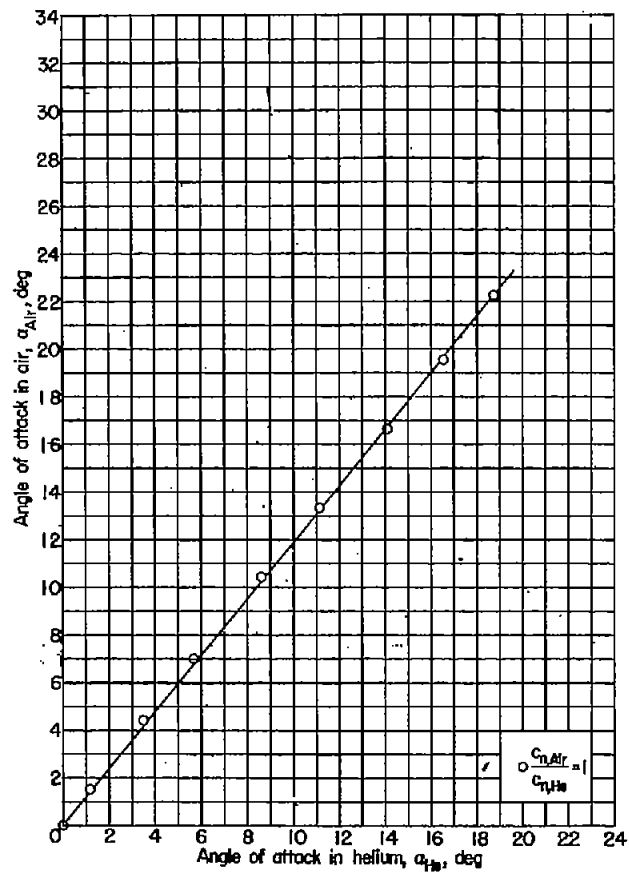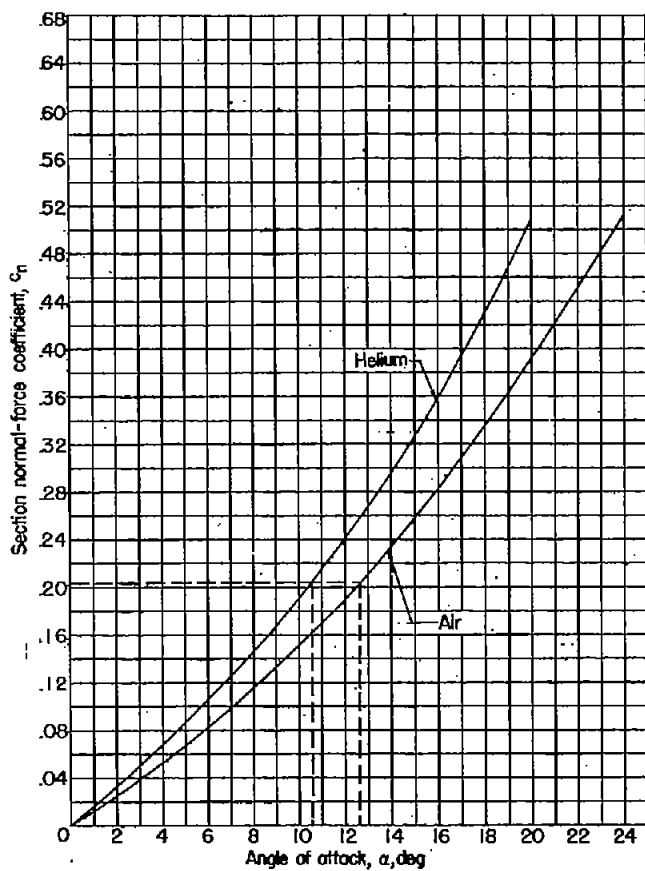
(b) $\theta = 15^{\circ}$.

Figure 8.- Continued.
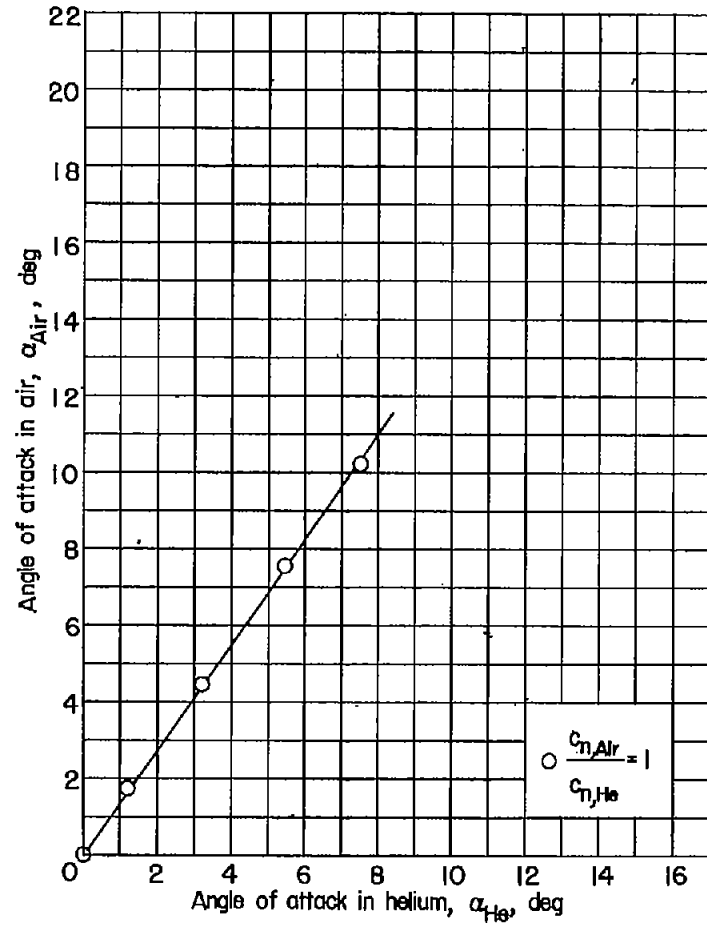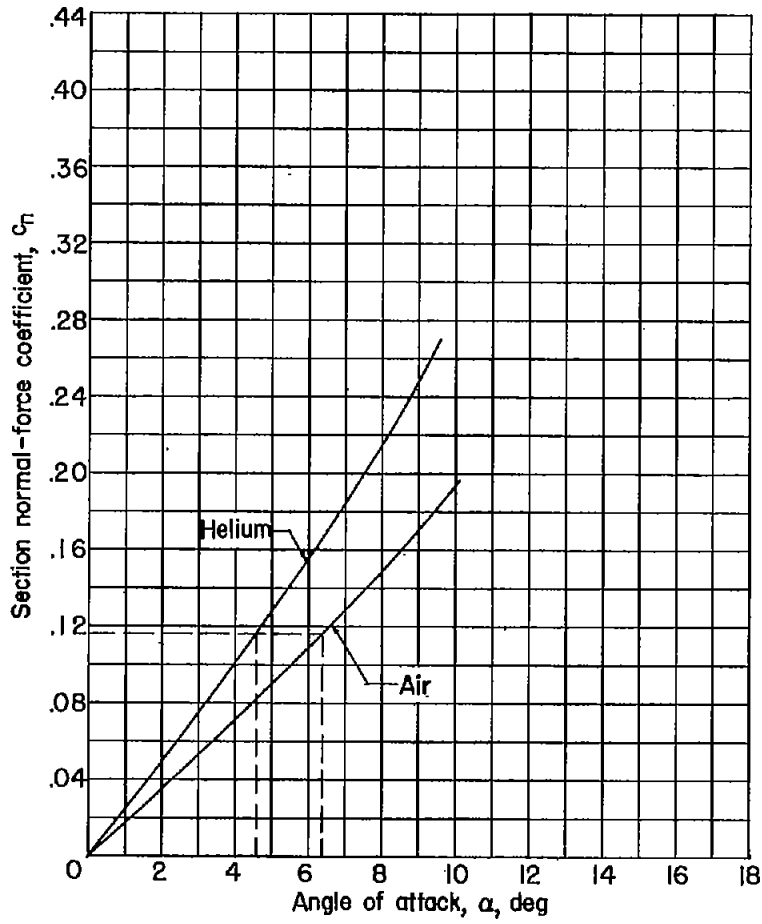
(c) θ = 27°.

Figure 8.- Concluded.
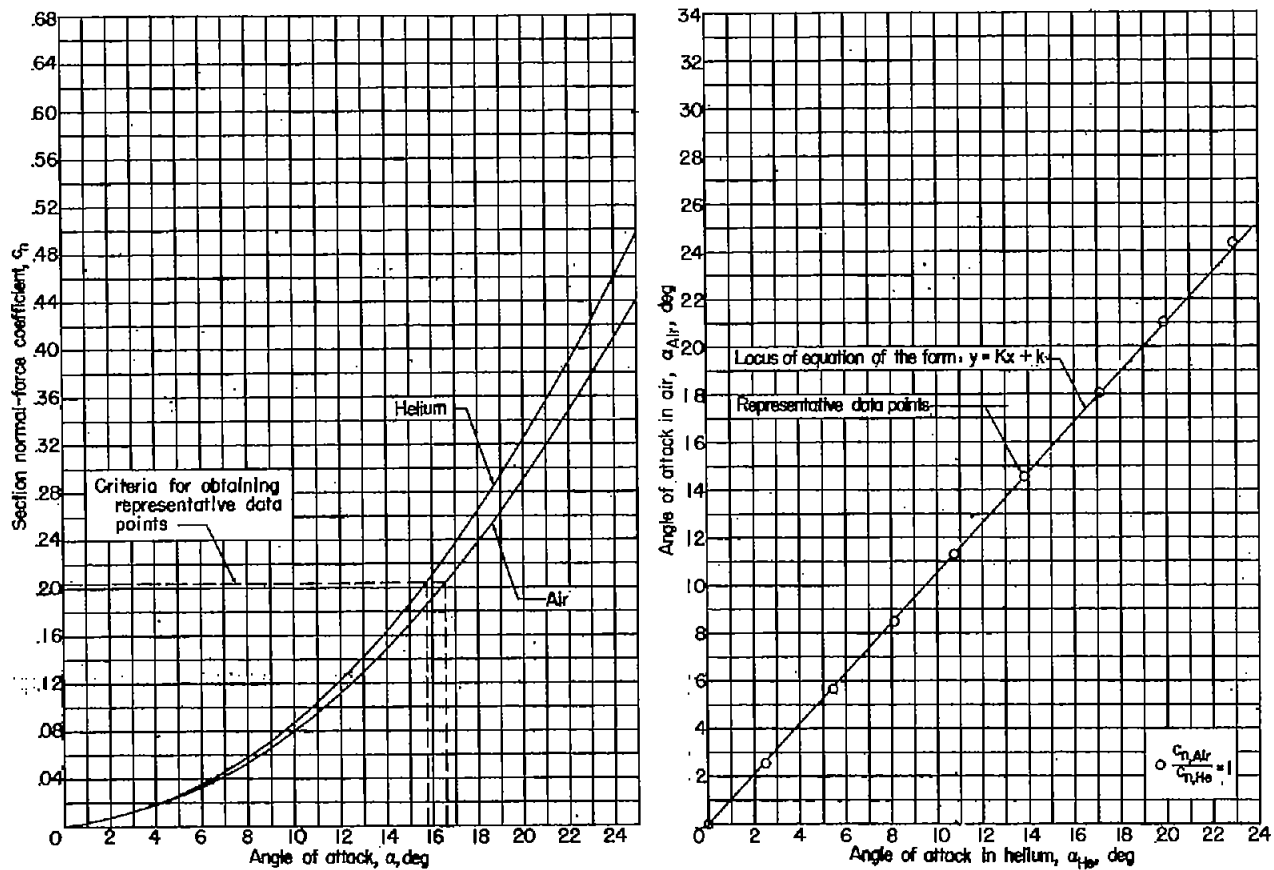
(a) $\theta = 0^{\circ}$ (flat plate).

Figure 9.- Variation of section normal-force coefficient c_n with angle
of attack α and variation of α_{Air} with α_{He} for $c_{n,Air}/c_{n,He} = 1$
for various half-angles at leading edge for wedge slab airfoil sections
at $M_{\infty} = 20$.

(b) $\theta = 15^O$.

Figure 9.- Continued.

(c) $\theta = 27^\circ$.
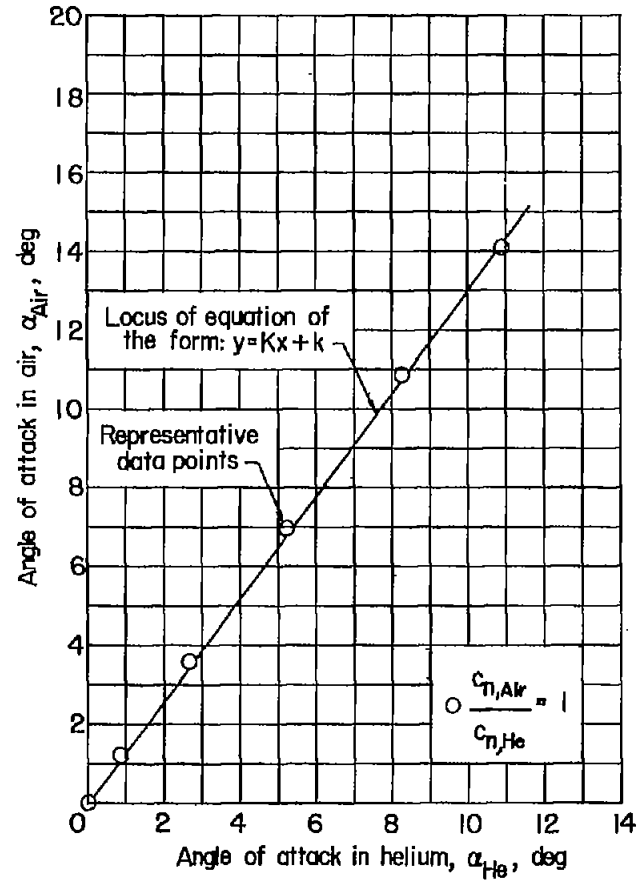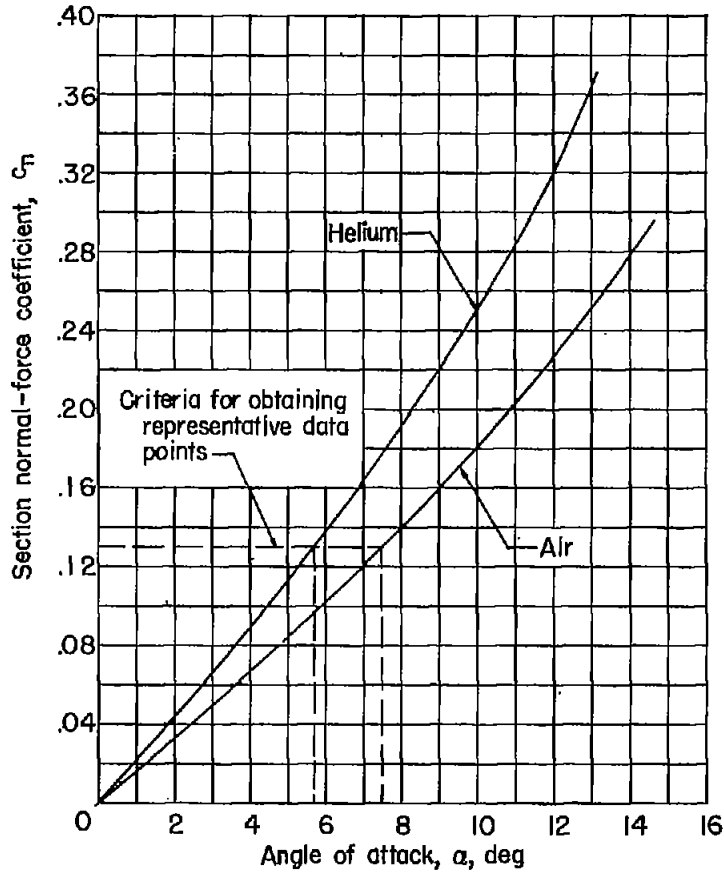
Figure 9.- Concluded.

(a) Wedge slab.

Figure 10.- Variation of section normal-force coefficient c_n with angle of attack α and variation of α_{Air} with α_{He} for $c_{n,Air}/c_{n,He} = 1$ for wedge slab and parabolic-arc slab airfoil sections. $M_{\infty} = 16$; $\theta = 11.27°$.
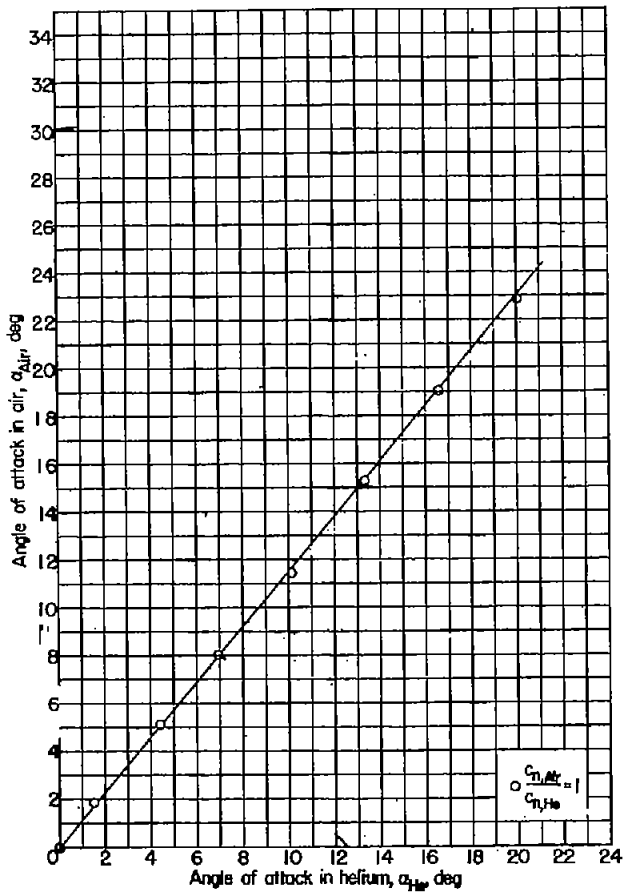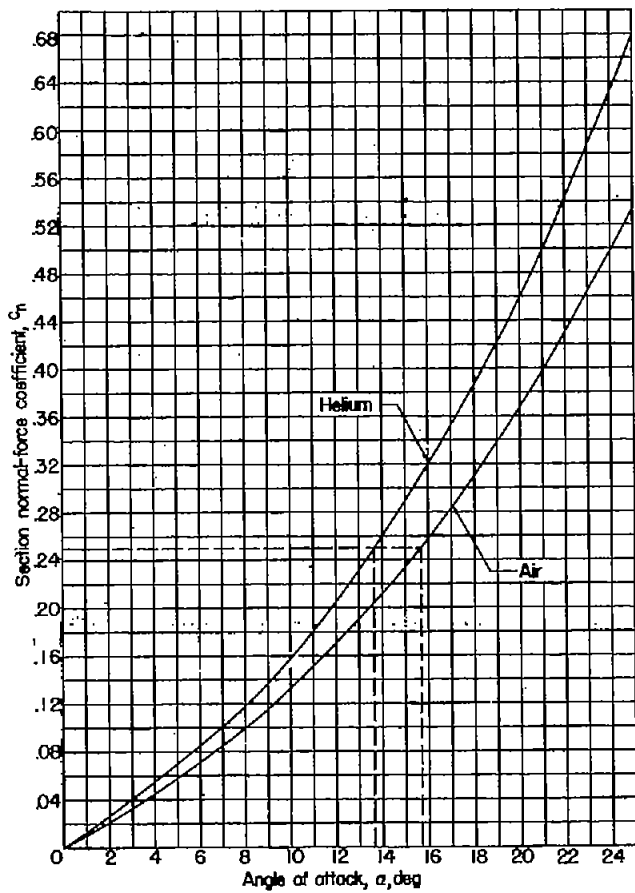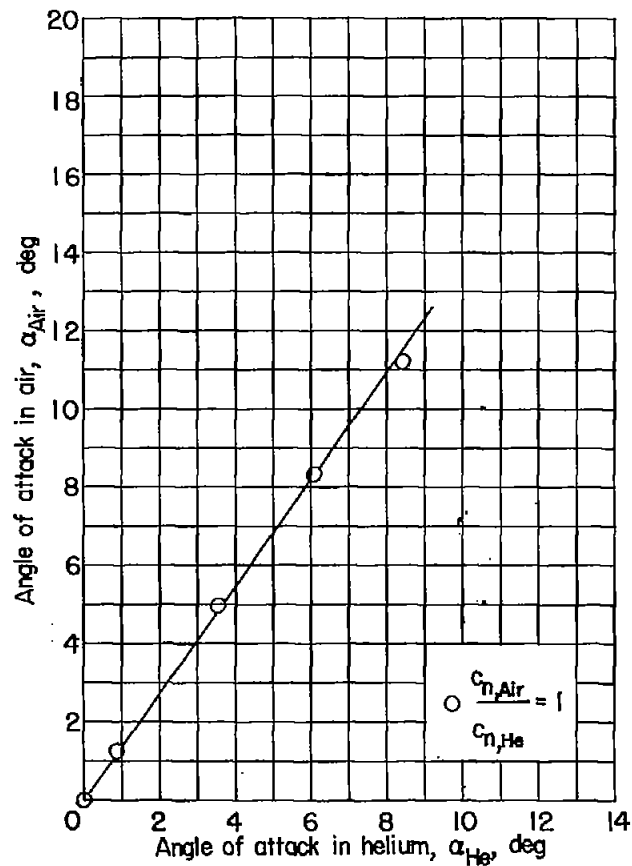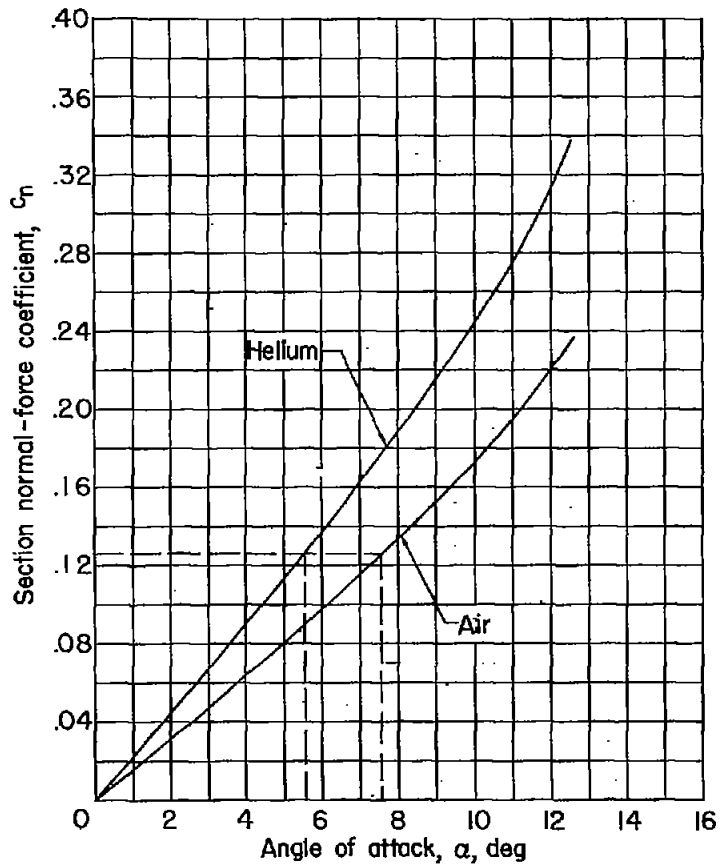
(b) Parabolic-arc slab.

Figure 10.- Concluded.

(a) Wedge slab.

Figure 11.- Variation of section normal-force coefficient c_n with angle of attack α and variation of α_{Air} with α_{He} for $c_{n,Air}/c_{n,He} = 1$ for wedge slab and parabolic-arc slab airfoil sections. $M_\infty = 16$; $\theta = 24.27^\circ$.

(b) Parabolic-arc slab.

Figure 11.- Concluded.

M_∞	Correlation factor, K										
	Half-angle at leading edge, θ, deg										
	0	3	9	11.27	11.27*	15	21	24.27	24.27*	27	30
12	1.05	1.07	1.12	1.14	1.15	1.18	1.25	1.30	1.31	1.37	1.47
16	1.05	1.07	1.13	1.15	1.15	1.19	1.26	1.30	1.37	1.38	1.50
20	1.05	1.07	1.12	1.15	1.16	1.18	1.26	1.33	1.33	1.40	1.51

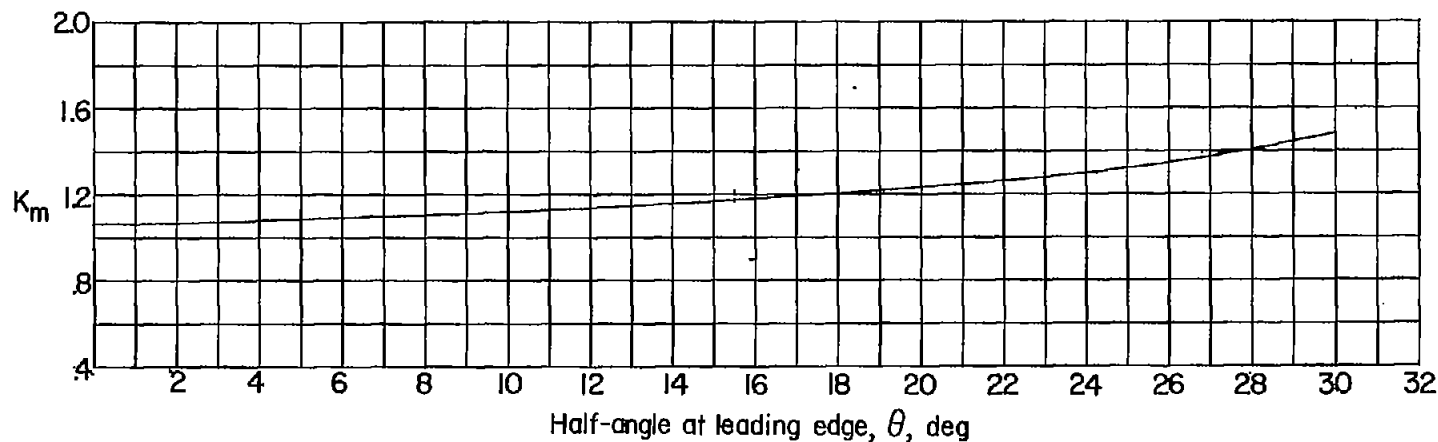*Indicates parabolic-arc slab sections

Figure 12.- Variation of correlation factor K and K_m with half-angle at leading edge for Mach numbers of 12, 16, and 20. (Wedge-slab configurations unless otherwise noted.) Thickness, 10 percent.